



UvA-DARE (Digital Academic Repository)

Primary root protophloem differentiation requires balanced phosphatidylinositol-4,5-biphosphate levels and systemically affects root branching.

Rodriguez-Villalon, A.; Gujas, B.; van Wijk, R.; Munnik, T.; Hardtke, C.S.

DOI

[10.1242/dev.118364](https://doi.org/10.1242/dev.118364)

Publication date

2015

Document Version

Final published version

Published in

Development - The Company of Biologists

License

Unspecified

[Link to publication](#)

Citation for published version (APA):

Rodriguez-Villalon, A., Gujas, B., van Wijk, R., Munnik, T., & Hardtke, C. S. (2015). Primary root protophloem differentiation requires balanced phosphatidylinositol-4,5-biphosphate levels and systemically affects root branching. *Development - The Company of Biologists*, 142(8), 1437-1446. <https://doi.org/10.1242/dev.118364>

General rights

It is not permitted to download or to forward/distribute the text or part of it without the consent of the author(s) and/or copyright holder(s), other than for strictly personal, individual use, unless the work is under an open content license (like Creative Commons).

Disclaimer/Complaints regulations

If you believe that digital publication of certain material infringes any of your rights or (privacy) interests, please let the Library know, stating your reasons. In case of a legitimate complaint, the Library will make the material inaccessible and/or remove it from the website. Please Ask the Library: <https://uba.uva.nl/en/contact>, or a letter to: Library of the University of Amsterdam, Secretariat, P.O. Box 19185, 1000 GD Amsterdam, The Netherlands. You will be contacted as soon as possible.

UvA-DARE is a service provided by the library of the University of Amsterdam (<https://dare.uva.nl>)

RESEARCH ARTICLE

Primary root protophloem differentiation requires balanced phosphatidylinositol-4,5-bisphosphate levels and systemically affects root branching

Antia Rodriguez-Villalon¹, Bojan Gujas¹, Ringo van Wijk², Teun Munnik² and Christian S. Hardtke^{1,*}

ABSTRACT

Protophloem is a specialized vascular tissue in growing plant organs, such as root meristems. In *Arabidopsis* mutants with impaired primary root protophloem differentiation, *brevis radix* (*brx*) and *octopus* (*ops*), meristematic activity and consequently overall root growth are strongly reduced. Second site mutation in the protophloem-specific presumed phosphoinositide 5-phosphatase *COTYLEDON VASCULAR PATTERN 2* (*CVP2*), but not in its homolog *CVP2-LIKE 1* (*CVL1*), partially rescues *brx* defects. Consistent with this finding, *CVP2* hyperactivity in a wild-type background recreates a *brx* phenotype. Paradoxically, however, while *cvp2* or *cvl1* single mutants display no apparent root defects, the root phenotype of *cvp2 cvl1* double mutants is similar to *brx* or *ops*, although, as expected, *cvp2 cvl1* seedlings contain more phosphatidylinositol-4,5-bisphosphate. Thus, tightly balanced phosphatidylinositol-4,5-bisphosphate levels appear essential for proper protophloem differentiation. Genetically, *OPS* acts downstream of phosphatidylinositol-4,5-bisphosphate levels, as *cvp2* mutation cannot rescue *ops* defects, whereas increased *OPS* dose rescues *cvp2 cvl1* defects. Finally, all three mutants display higher density and accelerated emergence of lateral roots, which correlates with increased auxin response in the root differentiation zone. This phenotype is also created by application of peptides that suppress protophloem differentiation, *CLAVATA3/EMBRYO SURROUNDING REGION 26* (*CLE26*) and *CLE45*. Thus, local changes in the primary root protophloem systemically shape overall root system architecture.

KEY WORDS: *Arabidopsis*, Auxin, CLE peptide, Lateral roots, Phosphoinositides, *CLE45*, *CLE26*

INTRODUCTION

Tap root systems, such as in the model plant *Arabidopsis thaliana* (*Arabidopsis*), consist of a principal primary root that branches through the formation of lateral roots (Osmont et al., 2007). The initiation of lateral root primordia occurs at the root tip, in the so-called differentiation zone of the root meristem, which continuously produces the different primary root tissues in a reiterative growth process from a distal stem cell niche (Tian et al., 2014; Van Norman et al., 2013). A fine-tuned balance between the creation of new cells by division and the gradual loss of their meristematic identity by differentiation maintains the root apical meristem (Bennett and

Scheres, 2010; Dello Ioio et al., 2008). The activity, i.e. the cell production rate of the root meristem and thus its size, is influenced by various local as well as shoot-derived long-distance cues. The latter include photosynthetic sugars and (at least in the juvenile plant) the plant hormone auxin, both of which are thought to be delivered by targeted transport mechanisms through the phloem vasculature (Kircher and Schopfer, 2012; Robert and Friml, 2009; Stadler et al., 2005; Swarup et al., 2001).

In *Arabidopsis* roots, the meristem produces a bilaterally symmetric vasculature, with a central xylem axis that is flanked by two phloem poles (Lucas et al., 2013; Miyashima et al., 2013). Each phloem pole comprises two distinct cell types: the sieve elements, which are the actual conductive cells of the phloem; and the companion cells, which provide essential metabolic functions to the enucleated sieve elements (Lucas et al., 2013). The early, initial phloem is called protophloem and is the first tissue to differentiate in the root meristem (Furuta et al., 2014; Rodriguez-Villalon et al., 2014). It reaches from close to the stem cell niche up into the maturation zone of the meristem, where its function is gradually taken over by the neighboring metaphloem (which differentiates once the protophloem is mature) (Fig. 1A). The protophloem is thus the terminal conduit that delivers photosynthates and other growth cues to the meristem, and is therefore crucial for its maintenance and activity (Depuydt et al., 2013; Lucas et al., 2013). Sieve element differentiation is a complex process during which nuclei are broken down and cell walls are thickened (Furuta et al., 2014; Rodriguez-Villalon et al., 2014; Truernit et al., 2012). Genetic studies in *Arabidopsis* have identified two genes that promote the commitment of precursor cells to the sieve element differentiation program (Rodriguez-Villalon et al., 2014; Truernit et al., 2012): *BREVIS RADIX* (*BRX*) and *OCTOPUS* (*OPS*). Both encode different plant-specific plasma membrane-associated proteins, which are expressed in the developing protophloem and polar localized at the root-ward (*BRX*) or shoot-ward (*OPS*) end of cells (Scacchi et al., 2009; Truernit et al., 2012). In both *brx*- and *ops*-null mutants, root meristem protophloem cells frequently fail to differentiate properly. These so-called ‘gap cells’ disrupt the continuity of the protophloem sieve element strands, resulting in reduced phloem cargo delivery to the meristem (Depuydt et al., 2013; Rodriguez-Villalon et al., 2014; Truernit et al., 2012). This manifests in, for example, a systemically reduced auxin response throughout the meristem (Gujas et al., 2012; Rodriguez-Villalon et al., 2014), which is likely responsible for its reduced activity and size, and thus the decreased overall root growth observed in the mutants. Recent studies suggest that *OPS* is a master regulator of the commitment to sieve element fate, because extra *OPS* dose or an *ops* gain-of-function allele can rescue *brx* defects and can overcome hyperactivity of the *BARELY ANY MERISTEM 3* (*BAM3*)-*CLAVATA3/EMBRYO SURROUNDING REGION 45* (*CLE45*) receptor-ligand module (Rodriguez-Villalon et al., 2014), a

¹Department of Plant Molecular Biology, University of Lausanne, Biophore Building, Lausanne CH-1015, Switzerland. ²Swammerdam Institute for Life Sciences, Section Plant Physiology, University of Amsterdam, Amsterdam 1098 XH, The Netherlands.

*Author for correspondence (christian.hardtke@unil.ch)

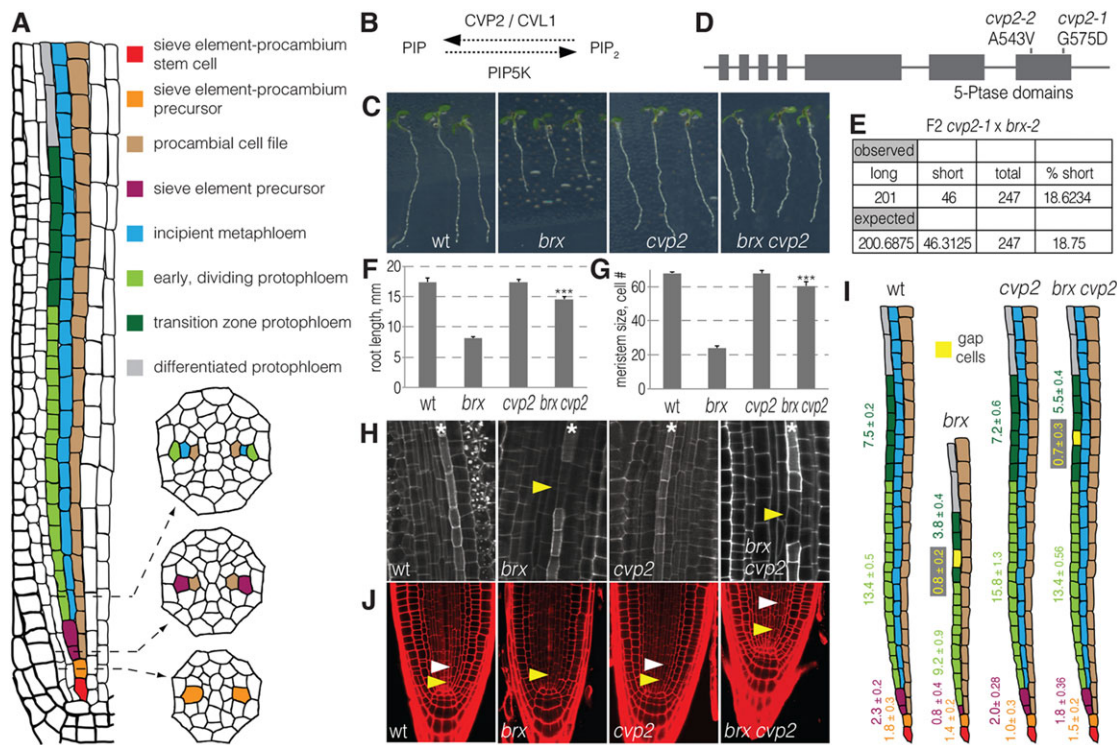


Fig. 1. Partial rescue of the *brx* mutant by *cvp2* second site mutation. (A) Schematic overview of protophloem development in the *Arabidopsis* root meristem. (B) Proposed enzymatic reaction catalyzed by CVP2 and its homolog CVL1, and the counter-reaction catalyzed by PIP5K. (C) Five-day-old seedlings of indicated genotypes (wt, wild type). (D) The molecular nature of the *cvp2* second site loss-of-function mutation (A543V). (E) Segregation of long-root and short-root phenotype individuals in a cross between the *brx-2*-null allele and another *cvp2* allele confirms second site rescue (no significant difference from expectation according to a Chi square test). (F,G) Root length (F) and mature meristem size (G) (expressed as number of meristematic cortex cells) of 5-day-old seedlings. Statistically significant differences are indicated with respect to wild-type or *brx* background. Error bars indicate s.e.m. *** $P < 0.001$ (Student's *t*-test). (H) Confocal microscopy images (grayscale) of 5-day-old propidium iodide (PI)-stained root meristems in the protophloem differentiation region. The protophloem sieve element strands (asterisks) stand out because of their enhanced PI staining. Arrowheads indicate gap cells. (I) Schematic qualitative-quantitative presentation of the stochastic phenotypes of the indicated mutants at 5 days (mean \pm s.e.m.). Color codes as in A. (J) Confocal microscopy images of 5-day-old PI-stained (red) root meristem tips. Yellow arrowheads indicate the first periclinal division of the sieve element-procambium precursor cell; white arrowheads indicate the second periclinal division of the sieve element precursor cell (absent in *brx*). Confocal microscopy images were obtained with a 63 \times magnification objective.

powerful inhibitor of sieve element specification that is de-regulated in *brx* roots (Depuydt et al., 2013).

Other genes involved in vascular development include *COTYLEDON VASCULAR PATTERN 2* (*CVP2*) and its partially redundant homolog *CVP2-LIKE 1* (*CVL1*), which encode phosphoinositide 5-phosphatases that presumably convert the cellular membrane signaling phospholipid phosphatidylinositol-4,5-bisphosphate (PIP₂) into phosphatidylinositol phosphates (PIPs) (Carland and Nelson, 2009, 2004; Munnik and Nielsen, 2011) (Fig. 1B). *CVP2* and *CVL1* have been originally characterized for the discontinuous vein pattern in cotyledons of the *cvp2* single and *cvp2 cvl1* double mutants (Carland and Nelson, 2009, 2004). In this study, we show that CVP2/CVL1-controlled PIP₂ levels have a specific role in root protophloem sieve element differentiation and need to be tightly regulated. We also find that disturbed primary root protophloem development systemically triggers increased lateral root density and accelerated lateral root emergence, thereby coupling primary root meristem activity to the shaping of overall root system architecture.

RESULTS

Second site mutation in *cvp2* partially rescues *brx* root growth defects

A specific role of *CVP2* in root protophloem sieve element differentiation was suggested to us by our finding that a second site

cvp2 mutation largely restores the root growth defects of a *brx*-null mutant (Fig. 1C). The *cvp2* allele isolated in our suppressor screen (Depuydt et al., 2013) has the same C to T base pair change that has been reported previously for the *cvp2-2* allele and results in CVP2 loss of function due to a crucial amino acid change: A543V (Carland and Nelson, 2004) (Fig. 1D). We thus recreated the double mutant by crossing *brx* to another loss-of-function allele, *cvp2-1* (Carland and Nelson, 2004), to confirm mutated *CVP2* as the causative suppressor locus (Fig. 1E). In *brx cvp2* double mutants, both overall root growth and meristem size are recovered to ~85% of wild type, from ~45% in *brx* single mutants (Fig. 1F,G). Concomitantly, undifferentiated gap cells still occur in the sieve element strands (Fig. 1H). However, because the size of the protophloem transition zone, where the crucial differentiation steps take place, is increased, the frequency of gap cells is approximately halved in *brx cvp2* double when compared with *brx* single mutants (Fig. 1I). The *cvp2* mutation also restores the missing periclinal sieve element precursor cell division, another hallmark secondary effect of impaired protophloem differentiation in *brx* mutants (Rodriguez-Villalon et al., 2014) (Fig. 1J). Finally, *cvp2* second site mutation also partially rescues the lateral root formation phenotype of *brx* (see below; supplementary material Fig. S1A). In summary, we conclude that *cvp2* mutation indeed suppresses both primary and secondary *brx* defects through its action in the protophloem, in line

with the highly protophloem-specific *CVP2* expression pattern (Rodríguez-Villalón et al., 2014).

***CVP2* hyperactivity impairs protophloem sieve element differentiation and overall root growth**

Suppression of *brx* defects by *cvp2* mutations suggests that skewed PIP₂ levels might be at least partially responsible for impaired protophloem sieve element differentiation. To test this notion, we

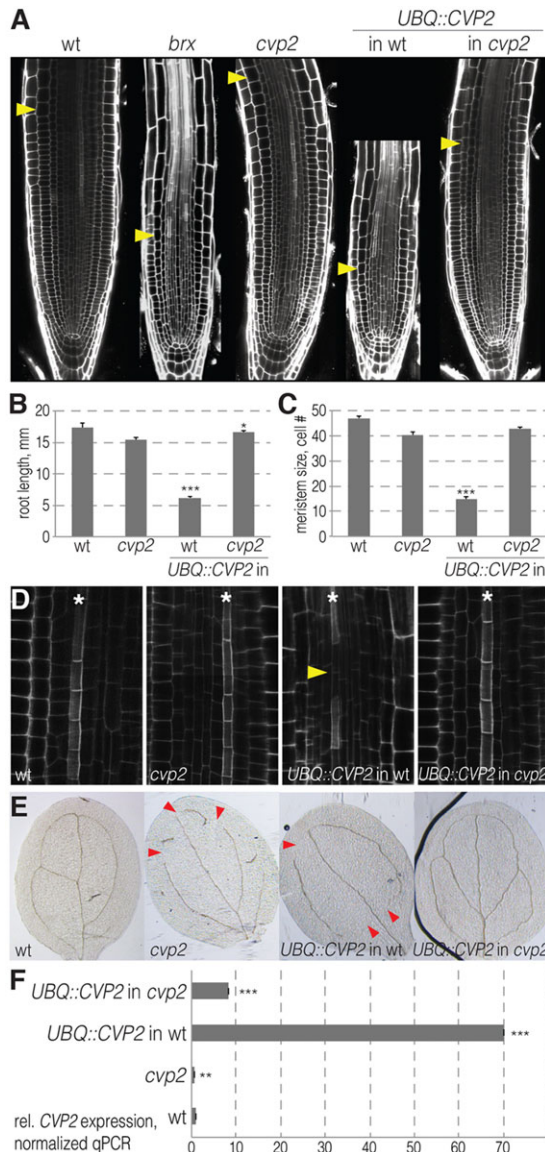


Fig. 2. *brx* root phenotype mimicked by *CVP2* overexpression.

(A) Confocal microscopy images (grayscale) of 5-day-old PI-stained root meristems of indicated mutant and transgenic genotypes. Arrowheads indicate the end of the meristematic zone (defined by the first rapidly elongating cortex cell) and thus root meristem size. (B-D) Corresponding root length (B), meristem size (C) and confocal microscopy images (D) in the protophloem differentiation region. Asterisks indicate protophloem sieve element strands. Arrowhead indicates gap cells. (E) Vascular cotyledon phenotypes (composite images obtained with a 5× magnification objective) of indicated genotypes in 7-day-old seedlings. Arrowheads indicate gaps in the vascular strand network. (F) qPCR quantification of *CVP2* expression levels in the roots of indicated genotypes, normalized with respect to the housekeeping gene *EF1* and relative to wild type (=1). Confocal microscopy images in A and D were obtained with a 63× magnification objective. Error bars indicate s.e.m. * $P < 0.05$; ** $P < 0.01$; *** $P < 0.001$ (Student's *t*-test).

constructed a transgene in which we combined the genomic region of the *CVP2* transcript with the *UBIQUITIN 10 (UBQ)* promoter. Although the *UBQ* promoter confers some level of ectopic expression throughout the root, it is comparatively strong in the developing protophloem with a peak in the transition zone (Santuari et al., 2011) and was thus ideally suited for our purpose. Strikingly, when introduced into wild-type plants, this *UBQ::CVP2* transgene induces a root phenotype that is similar to *brx* (or *ops*) mutants (Fig. 2A-D). Moreover, we observed a mild *cvp2*-like phenotype in the cotyledons of these plants, i.e. occasionally interrupted vascular strands (Fig. 2E). It appears unlikely that these phenotypes could, for example, arise from co-suppression, as *CVP2* transcript could be easily detected and was overexpressed up to 70-fold in the transgenic plants (Fig. 2F), and because the phenotypes are not observed when the transgene is introduced into *cvp2* loss-of-function point mutants. Rather, in this situation the transgene rescues the *cvp2* phenotype (Fig. 2E), underlining the quantitative impact of *CVP2* dose.

Second-site *cvl1* loss-of-function mutation does not suppress the defects of *brx* mutants

Although the *cvp2* mutation partially suppresses *brx* root phenotypes, the lack of *BRX* does not suppress the defective vascular pattern of *cvp2* cotyledons (Fig. 3), suggesting the existence of organ-specific mechanisms or (partial) gene redundancies in vasculature formation. For example, *cvl1* loss-of-function mutants display no discernible phenotypes by themselves (Carland and Nelson, 2009). This is consistent with the finding that, despite their 84% homology, the enzymatic activity of the CVL1 protein is lower than that of the *CVP2* protein. Together with its stronger expression, this suggests that *CVP2* is the dominant 5-phosphatase of the two (Carland and Nelson, 2009). Matching these observations, we did not observe phenotypic suppression in *brx cvl1* double mutants that we constructed (supplementary material Fig. S1B). However, *cvl1* loss-of-function enhances the foliar phenotypes of *cvp2* mutants (Carland and Nelson, 2009) (Fig. 3), again underlining the dose effect of overall 5-phosphatase activity.

cvp2 cvl1* double mutants display a root phenotype that is similar to *brx* and *ops

Next, we sought to investigate the possibly redundant role of *CVP2* and *CVL1* in the root. It has been reported that enzymes likely

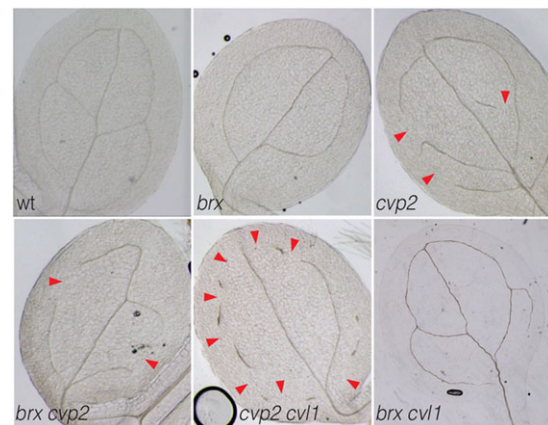


Fig. 3. Cotyledon vascular patterns. Vascular cotyledon phenotypes (composite images obtained with a 5× magnification objective) of indicated genotypes in 7-day-old seedlings. Arrowheads indicate gaps in the vascular strand network.

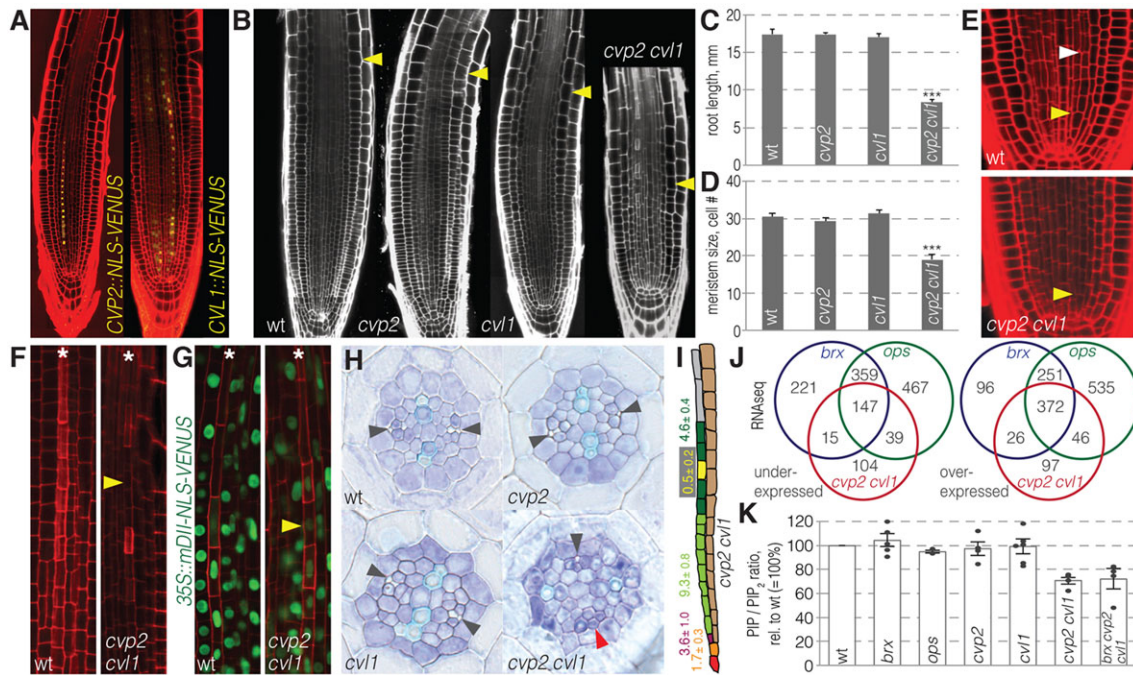


Fig. 4. Root phenotype of *cvp2 cvl1* mutants. (A) Expression patterns of *CVP2* and *CVL1*, as revealed by fluorescent NLS-VENUS reporter genes. PI staining indicates coincidence of expression with the developing protophloem. (B) Confocal microscopy images (grayscale) of 5-day-old PI-stained root meristems of indicated mutant genotypes. Arrowheads indicate the end of the meristematic zone. (C,D) Corresponding root length (C) and meristem size (D); significant differences are indicated with respect to wild-type background. (E) Confocal microscopy images of 5-day-old PI-stained (red) root meristem tips. Yellow arrowheads indicate first periclinal division of the sieve element-procambium precursor cell; white arrowhead indicates second periclinal division of the sieve element precursor cell (absent in *cvp2 cvl1*). (F) Corresponding images in the protophloem differentiation region. Asterisks indicate protophloem sieve element strands. Arrowheads indicate gap cells. (G) Confocal microscopy images of 5-day-old PI-stained (red) root meristem protophloem differentiation regions, overlap with mDII-VENUS nuclear marker (green). Asterisks indicate protophloem sieve element strands. Arrowhead indicates gap cell. (H) Toluidine Blue-stained histological cross-sections of roots at the position of differentiated protoxylem. Black arrowheads indicate the two protophloem sieve element cells; red arrowhead indicates an undifferentiated protophloem cell in *cvp2 cvl1*. (I) Schematic qualitative-quantitative presentation of the stochastic phenotypes of *cvp2 cvl1* mutants at 5 days. Color codes as in Fig. 1A. (J) Overlap of differentially expressed genes ($P < 0.001$) in 5-day-old roots of indicated genotypes when compared with wild type, determined by mRNA sequencing. (K) PIP/PIP₂ ratios in 6-day-old seedlings of indicated genotypes. The graph groups multiple replicate experiments, values have been normalized to their respective wild-type controls (=100%). Dots indicate measurements from individual replicates. Confocal as well as light microscopy images were obtained with a 63 \times magnification objective. Error bars indicate s.e.m. *** $P < 0.001$ (Student's *t*-test).

involved in PIP to PIP₂ forward and reverse interconversion are expressed in different root meristematic tissues (Carland and Nelson, 2004; Tejos et al., 2014), although a full cellular resolution analysis is still needed. Moreover, a short-root phenotype has been reported for *cvp2 cvl1* double mutants (Carland and Nelson, 2009). We have previously shown that a reporter gene expressing a nuclear-localized fluorescent VENUS reporter protein under control of the *CVP2* promoter (*CVP2::NLS-VENUS*) is specifically expressed in the developing protophloem of the root meristem (Rodriguez-Villalon et al., 2014) (Fig. 4A). Likewise, a *CVL1::NLS-VENUS* reporter is most prominently expressed in developing protophloem sieve elements, but also, albeit at a lower level, in the neighboring companion cell files and in the developing metaphloem (Fig. 4A). The notion of redundancy of the two genes in the root protophloem was confirmed by analysis of *cvp2 cvl1* double mutants. Although the roots of *cvp2* and *cvl1* single mutants are indistinguishable from wild-type plants with respect to meristem size, tissue organization and growth rate, the *cvp2 cvl1* double mutants display a root phenotype that is very similar to *brx* (or *ops*). It encompasses all aspects from strongly reduced meristem size and overall root growth, frequent occurrence of what appear to be gap cells specifically in the developing protophloem, and the associated frequent absence of the periclinal sieve element precursor cell division (Fig. 4B-F). To corroborate that gap cells in *cvp2 cvl1* mutants are also cells that fail to enter the sieve element differentiation program, we introduced the

nuclear marker mDII-NLS-VENUS expressed under the constitutive 35S promoter (Brunoud et al., 2012). Similar to *brx* and *ops*, the nucleus persists in *cvp2 cvl1* gap cells while their cell wall is thinner than in flanking cells (Fig. 4G), confirming that these cells fail to differentiate. Moreover, analysis of Toluidine Blue-stained cross-sections of *cvp2 cvl1* roots taken at the level of advanced protoxylem differentiation confirmed the frequent presence of undifferentiated cells in the protophloem position (Fig. 4H), a phenotype that was never observed in *cvp2* or *cvl1* single mutants. Finally, beyond these morphological similarities (summarized in Fig. 4I), we also monitored the transcriptome of young *brx*, *ops* and *cvp2 cvl1* roots by mRNA sequencing. In all three genotypes, several hundred genes showed differential expression (*brx*, 1487; *ops*, 2,216; *cvp2 cvl1*, 846) (supplementary material Tables S1-S3), and the majority of those genes in *cvp2 cvl1* (519 out of 846) were also differentially expressed in *brx* and *ops* (Fig. 4J) (see supplementary material Table S4 for a Gene Ontology analysis). Thus, the gene sets largely overlapped between the genotypes (pairwise overlap between all three mutants from 51% to 76%), once more corroborating the similarity of their root phenotypes.

***cvp2 cvl1* double mutants display a skewed PIP to PIP₂ ratio**

The PIP₂ conversion into PIP that is catalyzed by 5-phosphatases is mirrored by PIP 5-kinases that catalyze the inverse reaction, and it is conceivable that cross-regulatory mechanisms could result in

metabolite shifts that would reconcile the paradoxical *cvp2 cvl1* phenotype with those of the other lines. Thus, we set out to measure levels of these phosphoinositides in young seedling roots to verify that the *cvp2 cvl1* double mutant root phenotype is indeed associated with higher PIP₂ levels as would be expected (Carland and Nelson, 2009). Measurements of ³²P_i-incorporation into PIP and PIP₂ in wild-type and mutant seedlings indicate that the level of PIP₂ is indeed higher in *cvp2 cvl1* roots (in four out of four replicate experiments, on average 155.6±14.3% of wild-type control). To circumvent any artifacts due to systemic differences in ³²P_i uptake and developmental phenotypes, we also determined the relative changes of PIP₂ when compared with the more abundant PIP. Indeed, we found that in *cvp2 cvl1* double mutant roots, the PIP/PIP₂ ratio is skewed towards higher PIP₂ levels, again consistent with the reduced proposed enzymatic activity (Fig. 4K). The other mutants were also included in the measurements, and although occasionally elevated PIP₂ levels and a positively skewed PIP/PIP₂ ratio was observed in *brx* (but not in *ops*) mutants, the latter was not robust across experiments (Fig. 4K). Likewise, although higher PIP₂ levels were typically measured in *cvp2* single mutants (in four out of five replicate experiments, on average 117.7±4.5% of wild-type control), a negatively skewed PIP/PIP₂ ratio was not consistently observed. This could mean that smaller alterations are masked in the assay because the developing protophloem only represents a small fraction of the tissue sampled. However, matching the genetic data, the results also show that impaired root protophloem development and its secondary defects are not necessarily associated with detectable shifts in the PIP/PIP₂ ratio. Adding further genetic evidence to this, we also found that although *cvp2* mutation partially suppresses the *brx* phenotype, *cvl1* mutation does not (supplementary material Fig. S1B); in *brx cvp2 cvl1* triple mutants, the rescue is abolished (supplementary material Fig. S1B,C). These triple mutants thus display the same root phenotype as *brx*, *ops* or *cvp2 cvl1* mutants, and, similar to the latter, they display higher PIP₂ levels (in four out of five replicate experiments, on average 137.3±6.0% of wild-type control) and a consistently negatively skewed PIP/PIP₂ ratio (Fig. 4K).

CVP2 loss of function cannot rescue ops phenotypes, whereas increased OPS dose suppresses the cvp2 cvl1 double mutant phenotype

To test whether, similar to *brx cvp2* double mutants, *cvp2* second site mutation could partially or fully rescue *ops* defects, we constructed a *cvp2 ops* double mutant. These plants display a fully penetrant *ops* phenotype, suggesting that *cvp2* rescue is specific to *brx* and excluding the possibility that *cvp2* mutation can rescue impaired protophloem mutants through some type of systemic effect (Fig. 5A). In line with the latter conclusion, the root phenotype of *cvp2 cvl1* double mutants does not depend on the shoot genotype, as demonstrated through reciprocal grafting experiments (Fig. 5B). *OPS* has recently been described as the key regulator of commitment to protophloem sieve element fate, underlined by the finding that introduction of an *OPS::OPS-GFP* transgene can fully rescue the *brx* mutant phenotype (Rodríguez-Villalón et al., 2014). We thus tested whether the same is true for *cvp2 cvl1* double mutants. Indeed, introduction of *OPS::OPS-GFP* into *cvp2 cvl1* fully rescues the root phenotypes of the double mutant (Fig. 5A,C). Considering the persistence of the *ops* phenotype in a *cvp2 ops* double mutant and the rescue of *cvp2 cvl1* by extra *OPS* dose, the data thus suggest that *OPS* activity might be one of the key effectors of PIP₂ levels in the developing root protophloem.

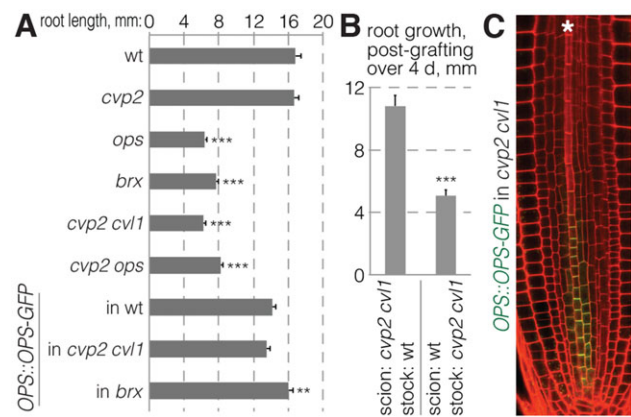


Fig. 5. Rescue of the *cvp2 cvl1* root phenotype by increased OPS dose. (A) Root length of 5-day-old seedlings of indicated mutant or transgenic genotype. Significant differences are indicated with respect to wild-type (mutants) or transgenic wild-type (transgenic lines) background. (B) Root growth measurements over 4 days after grafting 5-day-old shoot scions on indicated root stocks. Error bars indicate s.e.m. ** $P < 0.01$; *** $P < 0.001$ (Student's *t*-test). (C) Confocal microscopy image (obtained with a 63× magnification objective) of a PI-stained (red) root meristem from a 5-day-old *cvp2 cvl1* seedling that expresses an additional transgenic OPS-GFP (green) copy. Asterisk indicates protophloem sieve element strand.

Impaired protophloem differentiation systemically alters root system architecture

One characteristic of *brx* mutants is the association of the primary root phenotype with a seemingly more branched root system. This phenotype cannot be accounted for by slightly reduced mature cell length (a ~20% decrease in comparison to wild type) (Mouchel et al., 2004) and is observed in all three mutants (*brx*, *ops* and *cvp2 cvl1*). To investigate whether this phenotype possibly reflects a systemic effect of disturbed primary root protophloem differentiation, we embarked on a quantitative characterization of root branching in the mutants (Dubrovsky and Forde, 2012). Detailed analysis of their lateral root formation revealed that while the relative size of the *brx*, *ops* and *cvp2 cvl1* primary root meristem and the differentiation zone is comparable with wild type, the relative size of the mutants' lateral root formation zone is significantly smaller (Fig. 6A). Moreover, the relative size of their lateral root branching zone is increased (Fig. 6A) and displays a higher density of emerged lateral roots (Fig. 6B; supplementary material Fig. S1D). These observations suggest that, in all three mutants, lateral root initiation occurs more frequently and lateral root emergence is accelerated. To corroborate these results, we also scored the distribution of lateral root development stages (Malamy and Benfey, 1997; Péret et al., 2009). Early on (stages I–III), pericycle founder cells undergo asymmetric divisions to form a primordium, followed by anticlinal as well as periclinal divisions that enable its radial expansion. Once four cell layers are formed (stage IV), cells further expand and divide (stages V–VII), and the primordium eventually emerges as a lateral root from inside the primary root (stage VIII). We quantified the distribution of lateral root primordia developmental stages in all three genotypes according to this classification. At 7 days after germination, the majority of lateral root primordia in wild type are in their early stages (I–III; ~60%), and only a few lateral roots have emerged (stage VIII; ~20%) (Fig. 6C). In *brx*, *ops* and *cvp2 cvl1* mutants, the relative abundance of early stages is reduced while at the same time, 35–50% of lateral roots have already emerged (Fig. 6C). In summary, the results support the notion that a discontinuous protophloem progression not only reduces primary root growth, but also simultaneously increases

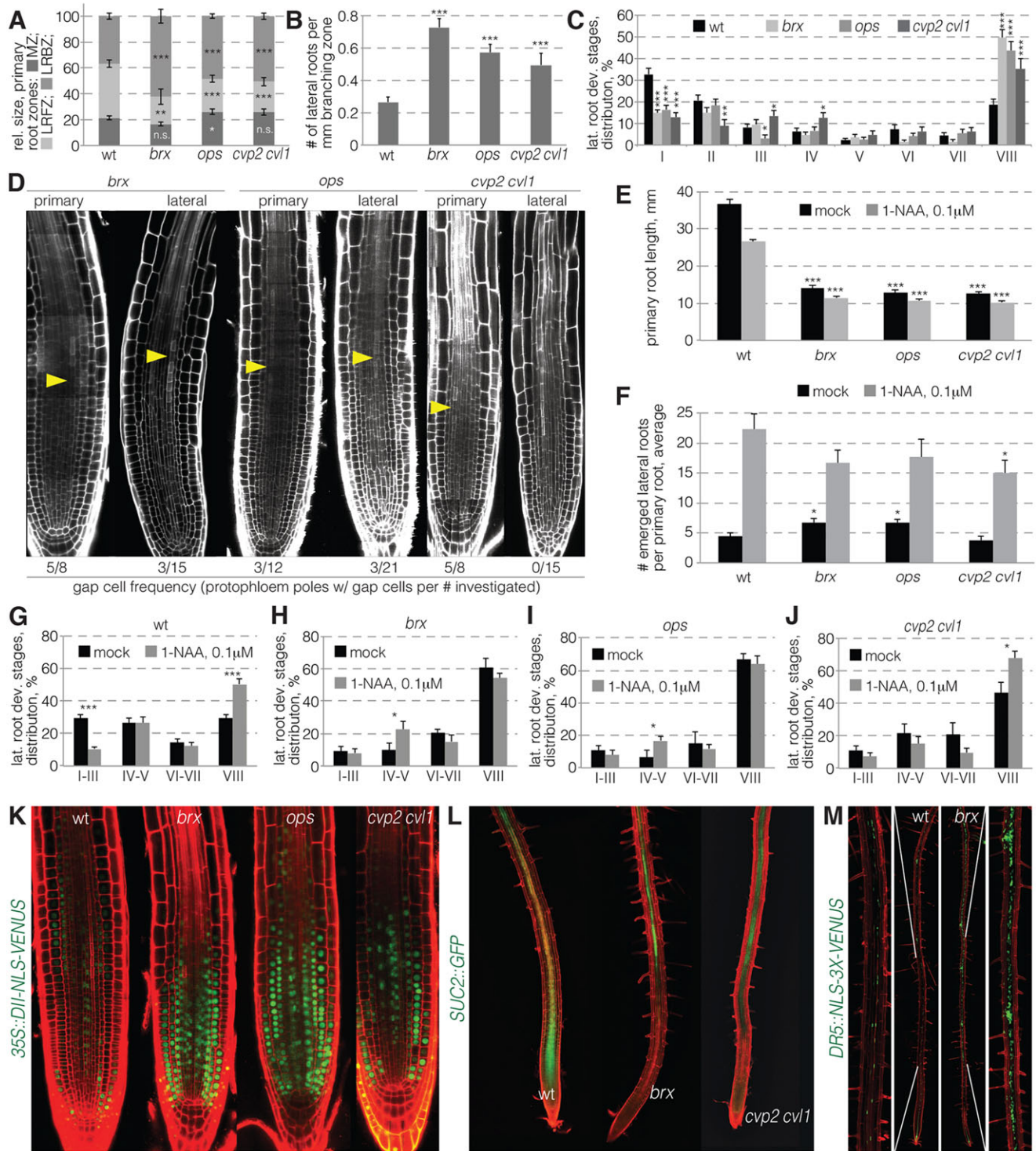


Fig. 6. Root-branching phenotypes and altered auxin activity distribution in protophloem differentiation mutants. (A-C) Seven-day-old seedlings of indicated genotypes were analyzed for: (A) average relative size of the meristem and differentiation zone (MZ), the lateral root formation zone (LRFZ) and the lateral root branching zone (LRBZ); (B) the corresponding density of emerged lateral roots in the LRBZ; and (C) the corresponding frequency of lateral root primordia stages (note stage VIII are emerged lateral roots). (D) Confocal microscopy images (grayscale) of 7-day-old PI-stained primary and lateral root meristems of indicated mutant genotypes. Arrowheads indicate gap cells. (E,F) Primary root length (E) and number of emerged lateral roots (F) in 7-day-old seedlings of indicated genotypes, grown on mock media for 4 days and then shifted onto mock conditions or on media containing the auxin analog 1-NAA for the following 3 days. (G-J) Frequency distribution of lateral root primordia stages in the seedlings assayed in E,F (stage VIII, emerged lateral roots). (K) Confocal microscopy images of PI-stained (red) root meristems of 5-day-old seedlings of indicated genotypes that constitutively express the fluorescent DII-VENUS inverse auxin activity reporter protein (green). (L) Confocal microscopy images of PI-stained (red) roots of 7-day-old seedlings of indicated genotypes that express free fluorescent GFP reporter protein (green) under the control of the companion cell-specific *SUC2* promoter. GFP unloading into the root meristem is strongly reduced in *brx* and *cvp2 cvl1* seedlings. (M) Confocal microscopy images of PI-stained (red) roots of 7-day-old wild-type and *brx* seedlings that carry the fluorescent DR5::NLS-3XVENUS auxin activity reporter (green) and flanking magnifications of the indicated differentiation zone regions. Confocal images in D and K were obtained with a 63× magnification objective, and in L and M with a 20× magnification objective. Error bars indicate s.e.m. Significant differences are indicated with respect to wild-type background or mock conditions. * $P < 0.05$; ** $P < 0.01$; *** $P < 0.001$ (Student's *t*-test).

lateral root formation. Notably, compared with the primary roots, the lateral roots of all three mutants display neither apparently reduced meristem size nor reduced growth rate. This correlates with the absence (*cvp2 cvl1*) or strong reduction in frequency (*brx* and *ops*) of protophloem gap cells in lateral root meristems (Fig. 6D).

Impaired protophloem differentiation systemically alters the auxin response pattern in the root system

The plant hormone auxin stimulates lateral root formation, and shoot-derived auxin is thought to be crucial for lateral root priming in *Arabidopsis* seedlings (Bhalerao et al., 2002; Van Norman et al., 2013). Indeed, application of the polar auxin transport inhibitor NPA suppresses lateral root formation not only in wild type, but also in the three mutants (supplementary material Fig. S1E,F). In wild type, application of the diffusible auxin analog 1-NAA not only leads to an increase in lateral root primordia density, but also accelerates lateral root emergence. Because at the same time primary root elongation is inhibited, this resembles the macroscopic phenotype observed for *brx*, *ops* and *cvp2 cvl1* roots in mock conditions. 1-NAA applications to *brx*, *ops* or *cvp2 cvl1* mutants also stimulate lateral root formation even further (Fig. 6E,F); however, only a slight (*cvp2 cvl1*) or no (*brx*, *ops*) effect on the proportion of emerged lateral roots was observed for the mutants (Fig. 6G-J). This might mean that in both mutants, endogenous auxin levels or activity are already high and are therefore saturated earlier. This notion contrasts with the previous finding that in *brx* mutants meristematic auxin response is reduced as indicated by the inverse auxin activity reporter *35S::DII-VENUS* (Gujas et al., 2012). Investigation of *ops* and *cvp2 cvl1* root meristems with this marker revealed equally decreased auxin activity (Fig. 6K), with overall lowest activity in *brx* and *ops* meristems, and an intermediate level in *cvp2 cvl1*. It has also been shown that protophloem sieve element discontinuity as in *brx* or *ops* results in strongly decreased phloem unloading into the meristem (Rodriguez-Villalon et al., 2014; Truernit et al., 2012). Again, with somewhat intermediate penetrance, this could also be observed in *cvp2 cvl1* double mutants (Fig. 6L). It thus appears possible that perturbed protophloem strand differentiation prevents efficient shoot-to-root meristem transfer of auxin, and might thus lead to enhanced accumulation of this hormone in the differentiation zone of the root and above, where lateral roots are formed. Because the DII-VENUS inverse marker is of limited use once auxin activity crosses a certain threshold (i.e. the marker is no longer detectable), we tested this hypothesis with *brx* as the prime example by introducing the fluorescent *DR5::NLS-3XVENUS* marker, an artificial reporter of auxin-induced transcription, into the mutant. Indeed, we found that, unlike in the *brx* root meristem tip, where *DR5* activity is reduced when compared with wild type, confirming previous results (Mouchel et al., 2006), *DR5* activity is actually higher from the differentiation zone upwards (Fig. 6M). Finally, to confirm the hypothesis independently in a situation that is not potentially distorted by ontogeny and therefore more directly comparable, we took advantage of the CLE45 and CLE26 peptides. CLE45 treatment suppresses the differentiation of newly formed root protophloem sieve elements and thus mimics the *brx* root meristem phenotype in all aspects (Depuydt et al., 2013; Rodriguez-Villalon et al., 2014). Similar to CLE45, CLE26 is expressed in the developing protophloem (Fig. 7A) and CLE26 treatment has a similar effect to CLE45 treatment (Fig. 7B). When wild-type plants that carry a *DR5::NLS-3XVENUS* transgene are treated with either CLE45 or CLE26, we could observe that in addition this leads to increased auxin response in the differentiation zone of the primary root and above (Fig. 7C). These effects could be observed within 48 h, a time

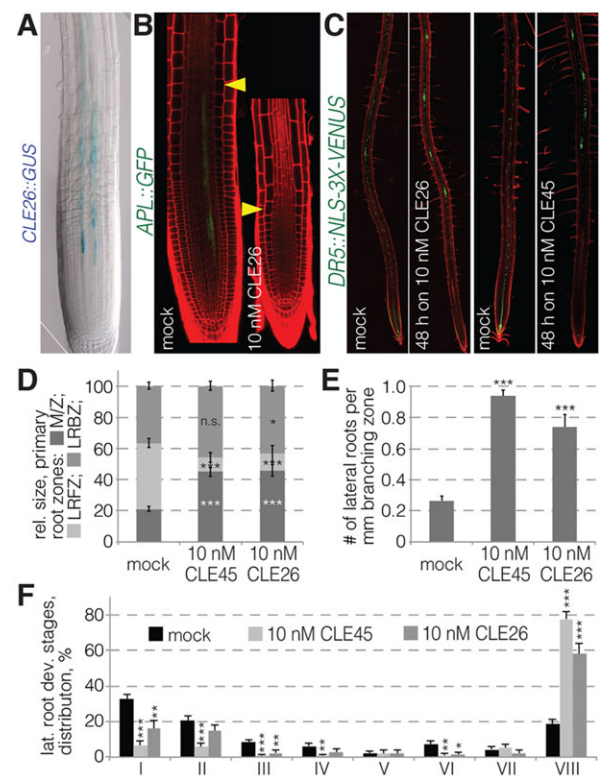


Fig. 7. Alteration of auxin activity distribution and enhancement of lateral root formation upon CLE26 or CLE45 treatment of wild-type roots. (A) Protophloem-specific expression of the *CLE26* gene, as revealed by a *CLE26::GUS* reporter gene. (B) Suppression of protophloem sieve element differentiation and thus primary root growth by CLE26 application. (C) Confocal microscopy images of PI-stained (red) roots of 6-day-old wild-type seedlings that constitutively express the fluorescent *DR5::NLS-3XVENUS* auxin activity reporter (green) grown on mock continuously, or shifted onto media containing CLE26 or CLE45 for 48 h after 4 days on normal media. (D-F) Seven-day-old seedlings grown on media with CLE26 or CLE45 were analyzed for: (D) average relative size of the meristem and differentiation zone (MZ), the lateral root formation zone (LRFZ) and the lateral root branching zone (LRBZ); (E) the corresponding density of emerged lateral roots in the LRBZ; and (F) the corresponding frequency of lateral root primordia stages (note stage VIII are emerged lateral roots). Confocal or light microscopy images were obtained with a 63× (A,B) or 20× (C) magnification objective. Error bars indicate s.e.m. Significant differences are indicated with respect to mock conditions. * $P < 0.05$; ** $P < 0.01$; *** $P < 0.001$ (Student's *t*-test).

window in which the formation of new protophloem is efficiently suppressed (Rodriguez-Villalon et al., 2014) while there is still little effect on overall root growth. When wild type is grown continuously on CLE26 or CLE45, the reduction of primary root growth (supplementary material Fig. S1D) is associated with a dramatic reduction in the relative size of the lateral root formation zone (Fig. 7D). At the same time, the density of lateral roots in the branching zone is increased (Fig. 7E) and their emergence is accelerated (Fig. 7F), mimicking the *brx*, *ops* and *cvp2 cvl1* mutant root system features. In summary, these results suggest that impaired protophloem sieve element differentiation indeed leads to increased auxin response in the more mature parts of the primary root and to the associated effects on lateral root formation.

DISCUSSION

PIP₂ levels are a crucial determinant in the progression of protophloem development

Phosphoinositides and their signaling roles were originally discovered in yeast and animals, where they have been implicated

in panoply of processes and regulatory functions (Balla, 2013). Although most enzymatic and regulatory proteins that have been shown to be involved in phosphoinositide turnover and signaling are conserved across the eukaryotes, their cellular and developmental roles in plants remain comparatively obscure to date (Boss and Im, 2012; Ischebeck et al., 2014). However, recent data suggest that PIP and PIP₂ are indeed signaling molecules in plants (Munnik and Nielsen, 2011). Isolation of the causal *cvp2* mutant alleles provided some of the first evidence for a developmental role of phosphoinositides (Carland and Nelson, 2009, 2004). In this context, our data support the notion that PIP₂ is the genuine substrate of CVP2/CVL1 (Carland and Nelson, 2009). The interrupted vascular bundles of *cvp2* (Carland and Nelson, 2004) and enhancement of the phenotype by *cvl1* in double mutants (Carland and Nelson, 2009) clearly implicated 5-phosphatases in vascular development and matched the vascular expression of a PIP 5-kinase gene (*PIP5K*), which catalyzes the proposed opposite reaction (PIP to PIP₂ conversion) (Elge et al., 2001). Similar to 5-phosphatases, the *PIP5K* genes are a family for which developmental roles are only about to emerge. For example, recently it has been reported that *pip5k1 pip5k2* double mutants display severely reduced root growth and interrupted foliar vasculature (Ischebeck et al., 2014; Tejos et al., 2014), similar to our transgenic *CVP2* overexpression lines. It will therefore be interesting to determine whether protophloem differentiation is impaired in *pip5k1 pip5k2* double mutants as well as in *pip5k1* single mutants (which already display reduced primary root growth).

In summary, the reported macroscopic phenotype of *pip5k1 pip5k2* double mutants corroborates the effects we observe upon *CVP2* over-expression and the partial suppression of *brx* phenotypes by *cvp2* second site mutation. Although a positively skewed PIP to PIP₂ ratio could be measured in older, whole *pip5k1 pip5k2* seedlings when PIP₂ levels were determined by quantifying the associated fatty acids by gas chromatography and mass spectrometry (Ischebeck et al., 2014), this could not be detected in *pip5k1 pip5k2* double mutant roots with the same experimental approach using labeling as in this study (Tejos et al., 2014). This suggests that the effect is too small and too localized, and could therefore be masked by the small relative abundance of the pertinent tissue. Likewise, a skewed PIP to PIP₂ ratio could not be consistently detected in *cvp2* single mutant roots. However, we found that *cvp2 cvl1* double mutant roots display a robust negatively skewed PIP to PIP₂ ratio, as could be expected. This observation creates a paradox, because the *cvp2 cvl1* root phenotype is similar to the one observed in *brx* or *ops* mutants and in *CVP2* overexpression lines. The most parsimonious interpretation of the data is therefore that a tightly regulated PIP₂ level is essential for proper protophloem differentiation and that shifting this level above or below a certain threshold creates a similar developmental phenotype.

The systemic effects of impaired protophloem development

It is noteworthy that compared with *brx* and *ops*, the *cvp2 cvl1* phenotype is somewhat intermediate, which is also reflected in its milder transcriptomic signature. Yet the fact that ~70% of the 846 genes that showed differential expression in *cvp2 cvl1* roots when compared with wild type are included in the corresponding *brx* and *ops* data sets underlines the similarity of the phenotypes and supports the notion that they represent a continuum of phenotypic severity. It is also conceivable that the transcriptome differences between the three mutants arise from the differences between the upper parts of their root systems. Although lateral roots had not yet emerged from the sampled 5-day-old primary roots, the different

dynamics of lateral root formation in the three genotypes suggests that corresponding developmental differences could already be present. Moreover, unlike *cvp2 cvl1*, both *brx* and *ops* lateral root meristems display mild protophloem differentiation defects, which further accentuates ontogenetic differences. The occurrence of none, or more or less severe defects in the lateral root meristems could reflect the different levels of potential redundancy in the different gene families. Whereas the 5-phosphatases in *Arabidopsis* comprise 15 genes (Carland and Nelson, 2009), only one of the four *BRX-LIKE* genes of *Arabidopsis* can fully substitute for *BRX* when expressed ectopically (Beuchat et al., 2010; Briggs et al., 2006), and it remains to be determined whether a functional homolog of *OPS* exists among the four *OPS-LIKE* genes (Nagawa et al., 2006; Truernit et al., 2012).

The quantitative differences notwithstanding, the overall root architecture of the three mutants is qualitatively very similar, with a higher initiation rate and accelerated emergence of lateral roots leading to a more branched root system. Our experiments suggest that this is likely the consequence of higher auxin activity starting from the differentiation zone of the primary root upwards. This contrasts with reduced auxin activity in the meristems, and a straightforward explanation for this phenomenon would be an auxin ‘traffic jam’ in the upper parts of the root, created from phloem-transported auxin that cannot be efficiently delivered to the meristem. To what degree phloem-transported auxin directly contributes to lateral root formation in the wild-type situation remains unclear (Swarup et al., 2001). However, it is conceivable that the dynamic feedback regulation of auxin transport could lead to a lateral redistribution of auxin once the path towards the meristem is constrained, as in the mutants. The occurrence of lateral roots that are not formed at the xylem pole, but elsewhere around the stele circumference in *brx* mutants (B.G., unpublished observations) is consistent with this idea. The observation that a shift in local auxin activity and associated root branching can also be triggered by treatment with peptides that suppress primary root protophloem differentiation also supports this notion. This interpretation also matches the previous observations that auxin efflux carrier abundance is reduced in the meristems of *brx* mutants (Scacchi et al., 2010) and that *brx* seedlings contain more free auxin per fresh weight (Sankar et al., 2011). It is also consistent with the proposed influence of the PIP to PIP₂ ratio on auxin efflux carrier polarization and plasma membrane abundance (Ischebeck et al., 2014; Tejos et al., 2014). It thus appears possible that locally disturbed polar auxin transport interferes with protophloem sieve element differentiation. A more general influence of PIP to PIP₂ ratio on cell polarity and membrane targeting could explain why *OPS* activity is genetically downstream of *CVP2/CVL1* action in the protophloem. Whether *OPS* polarity is indeed affected in *cvp2 cvl1* mutants could not be conclusively tested so far, as extra *OPS* dose rescues the *cvp2 cvl1* mutant phenotype. An inactive, yet correctly targeted *OPS* variant would be needed to address this issue. Finally, as auxin is thought to activate proton pumps, the ‘auxin traffic jam’ scenario would also be consistent with the reported proton pump hyperactivity of *brx* roots, the proposed adaptive feature that is responsible for the rare occurrence of *brx*-null mutants in natural *Arabidopsis* populations (Gujas et al., 2012).

MATERIALS AND METHODS

Plant tissue culture and molecular biology experiments, such as plant transformation, genomic DNA isolation, genotyping or sequencing were performed according to standard procedures as described previously (Scacchi et al., 2010).

Plant materials and growth conditions

All *Arabidopsis* lines were in the Col-0 wild-type background. The *cvp2-1*, *cvl1-1*, *cvp2 cvl1*, *ops-2* and *brx-2* mutant null alleles used in this study, and the *35S::DII-VENUS*, *35S::mDII-VENUS*, *CVP2::NLS-VENUS*, *SUC2::GFP* and *APL::GFP* reporter genes have been previously described (Brunoud et al., 2012; Carland and Nelson, 2009; Gujas et al., 2012; Scacchi et al., 2010; Truernit et al., 2012). The *brx-2 cvp2-2* double mutant obtained from the suppressor screen was backcrossed to Col-0 wild type twice before being used in our analyses. The *DR5::NLS-3XVENUS* and *CLE26::GUS* reporter genes were generously provided by Drs J. Vermeer (University of Lausanne, Switzerland) and J. Fletcher (University of California, Berkeley, USA).

Reporter constructs

To obtain the *CVL1::NLS-3XVENUS* reporter gene, a 2 kb genomic DNA fragment upstream of the *CVL1* start codon was amplified using oligonucleotides 5'-ATT GGT ACC GCA CAT CAC ATT GAT TT-3' and 5'-ATT CCC GGG TCT TGC TCT TAT TTG ATT C-3'. After *KpnI-XmaI* restriction enzyme digest, the fragment was cloned into a modified P4-P1r vector to generate the Gateway pENTRY-*pCVL1* plasmid. In addition the pENTRY *3XNLS-VENUS* vector was recombined into the pD091 vector to generate *CVL1::NLS-3xVENUS*. To create *UBQ::CVP2*, a 1.5 kb fragment of the genomic DNA region encoding *CVP2* was amplified using oligonucleotides 5'-GAA GAT CTT CGC CCA TCT TCA TGG AAT TAAAAGC-3' and 5'-GAA CTA GTC CGC GAA TTT GTG TGT TTC TAG-3', and recombined with the pENTRY-*UBQ* promoter clone into the pH7m24GW plasmid.

Hormone and CLE peptide treatments

For treatments, seedlings were grown on vertical plates with 0.5× MS salts, 1% sucrose, 1% agar, supplemented with 0.1 μM 1-NAA (Sigma), 5 μM NPA (Sigma), 10 nM CLE26 or 10 nM CLE45 as indicated. Unmodified CLE peptides were obtained by custom peptide synthesis (Genscript), dissolved in sterile nanopure water and diluted in autoclaved solid culture media. To perform short 1-NAA, NPA or CLE peptide treatments, plants were first grown under mock conditions and then transferred to plates supplemented accordingly.

Microscopy and histological analysis

To visualize meristems, roots were stained with 10 μg/ml PI and imaged by confocal (Zeiss LSM 510 instrument) or two-photon (Zeiss LSM 710 NLO instrument) microscopy. This method highlights root protophloem strands, which stain stronger than the surrounding tissues. GUS staining and light microscopy were performed according to standard procedures using a compound microscope (Leica 5500 instrument). For visualization of cotyledon vascular patterning, cotyledons of 7-day-old plants were prepared as previously described (Carland and Nelson, 2004) and imaged with a compound microscope. For primary root cross-sections, 5-day-old seedlings were fixed, embedded in Histo-resin (Leica Instruments GmbH) and sectioned on a microtome (Leica instrument) as described previously (Rodriguez-Villalon et al., 2014). Sections were mounted on slides, stained with Toluidine Blue for 2 min and visualized by light microscopy. Lateral root density and lateral root primordia were quantified as described previously (Dubrovsky et al., 2006; Dubrovsky and Forde, 2012). Briefly, seedlings were incubated at 62°C for 40 min in a 0.24 N HCl and 20% methanol solution, then at room temperature for 20 min in a 7% NaOH and 60% ethanol solution. Roots were then rehydrated via subsequent incubations in 40%, 20% and 10% ethanol, and finally in 25% glycerol diluted in 5% ethanol (2 h per step). Seedlings were mounted on slides with 50% glycerol and analyzed immediately by Nomarski optics with a compound microscope 40× magnification objective. A modified protocol in which roots were cleared in chloral hydrate solution instead was used to assess lateral roots in the 1-NAA-treated seedlings.

RNA-sequencing and qPCR

For mRNA sequencing, 5-day-old roots of the different genotypes grown in parallel on vertical plates were harvested and frozen in liquid nitrogen before

total RNA extraction was performed using a QIAGEN RNeasy Plant Kit. cDNA synthesis, amplification, size selection, high-throughput sequencing and bioinformatics analysis was performed as described previously (Depuydt et al., 2013). For pPCR quantification of *CVP2* (trans)gene expression, the following oligonucleotides were used: 5'-GCA ACA ATG AGA GAA GAG AAA TCC AAG-3' and 5'-CTC CCA GTT CTT ACT GAG TTT CTC AGT T-3'. *CVP2* expression was normalized with respect to the housekeeping gene *ELONGATION FACTOR 1 (EF1)*, monitored with oligonucleotides 5'-GGT CAC CAA GGC TGC AGT GAA GAA-3' and 5'-GCT CAA ACG CCA TCA AAG TTT TAA GAA-3'.

Phosphoinositide measurements

PIP and PIP₂ content was measured as previously described (Munnik and Zarza, 2013). Briefly, 5-day-old seedlings were incubated overnight with 10 μCi of carrier-free ³²P-labeled orthophosphate (three seedlings per sample, in triplicate). After ~16 h, lipids were extracted, separated and quantified by phosphoimaging.

Micrografting

Grafting between hypocotyls of *cvp2 cvl1* mutant scions and Col-0 wild-type stocks (or vice versa) using 5-day-old seedlings grown on plates at 25°C in 16 h light period was performed in tissue culture as previously described (Ragni et al., 2011). Four days after grafting, root growth of successfully grafted seedlings was measured.

Acknowledgements

We thank our colleagues Drs F. Carland, J. Fletcher and J. Vermeer for mutant, reporter line and plasmid gifts; Drs Y.-H. Kang and S. Depuydt for the initial isolation of the *brx cvp2* second site suppressor line; Dr M. Sankar for bioinformatics analysis of the mRNAseq data; and A. Breda for the *35S::DII-VENUS* in *ops* mutant background line.

Competing interests

The authors declare no competing or financial interests.

Author contributions

A.R.-V., B.G. and C.S.H. designed experiments and analyzed data, except for the phosphoinositide measurements (described in Fig. 4K), which were designed, performed and analyzed by R.v.W. and T.M. A.R.-V. and B.G. performed all other experiments. A.R.-V., T.M. and C.S.H. wrote the paper.

Funding

This work was supported by a Swiss National Science Foundation grant [310030B_147088] awarded to C.S.H. and by an EMBO Long Term Post-Doctoral Fellowship awarded to A.R.-V.

Supplementary material

Supplementary material available online at <http://dev.biologists.org/lookup/suppl/doi:10.1242/dev.118364/-/DC1>

References

- Balla, T. (2013). Phosphoinositides: tiny lipids with giant impact on cell regulation. *Physiol. Rev.* **93**, 1019-1137.
- Bennett, T. and Scheres, B. (2010). Root development—two meristems for the price of one? *Curr. Top. Dev. Biol.* **91**, 67-102.
- Beuchat, J., Li, S., Ragni, L., Shindo, C., Kohn, M. H. and Hardtke, C. S. (2010). A hyperactive quantitative trait locus allele of *Arabidopsis* BRX contributes to natural variation in root growth vigor. *Proc. Natl. Acad. Sci. USA* **107**, 8475-8480.
- Bhalerao, R. P., Eklöf, J., Ljung, K., Marchant, A., Bennett, M. and Sandberg, G. (2002). Shoot-derived auxin is essential for early lateral root emergence in *Arabidopsis* seedlings. *Plant J.* **29**, 325-332.
- Boss, W. F. and Im, Y. J. (2012). Phosphoinositide signaling. *Annu. Rev. Plant Biol.* **63**, 409-429.
- Briggs, G. C., Mouchel, C. F. and Hardtke, C. S. (2006). Characterization of the plant-specific BREVIS RADIX gene family reveals limited genetic redundancy despite high sequence conservation. *Plant Physiol.* **140**, 1306-1316.
- Brunoud, G., Wells, D. M., Oliva, M., Larrieu, A., Mirabet, V., Burrow, A. H., Beeckman, T., Kepinski, S., Traas, J., Bennett, M. J. et al. (2012). A novel sensor to map auxin response and distribution at high spatio-temporal resolution. *Nature* **482**, 103-106.
- Carland, F. M. and Nelson, T. (2004). Cotyledon vascular pattern2-mediated inositol (1,4,5) triphosphate signal transduction is essential for closed venation patterns of *Arabidopsis* foliar organs. *Plant Cell* **16**, 1263-1275.

- Carland, F. and Nelson, T.** (2009). CVP2- and CVL1-mediated phosphoinositide signaling as a regulator of the ARF GAP SFC/VAN3 in establishment of foliar vein patterns. *Plant J.* **59**, 895-907.
- Dello Iorio, R., Nakamura, K., Moubayidin, L., Perilli, S., Taniguchi, M., Morita, M. T., Aoyama, T., Costantino, P. and Sabatini, S.** (2008). A genetic framework for the control of cell division and differentiation in the root meristem. *Science* **322**, 1380-1384.
- Depuydt, S., Rodriguez-Villalon, A., Santuari, L., Wyser-Rmili, C., Ragni, L. and Hardtke, C. S.** (2013). Suppression of Arabidopsis protophloem differentiation and root meristem growth by CLE45 requires the receptor-like kinase BAM3. *Proc. Natl. Acad. Sci. USA* **110**, 7074-7079.
- Dubrovsky, J. G. and Forde, B. G.** (2012). Quantitative analysis of lateral root development: pitfalls and how to avoid them. *Plant Cell* **24**, 4-14.
- Dubrovsky, J. G., Gambetta, G. A., Hernández-Barrera, A., Shishkova, S. and González, I.** (2006). Lateral root initiation in Arabidopsis: developmental window, spatial patterning, density and predictability. *Ann. Bot.* **97**, 903-915.
- Elge, S., Brearley, C., Xia, H.-J., Kehr, J., Xue, H.-W. and Mueller-Roeber, B.** (2001). An Arabidopsis inositol phospholipid kinase strongly expressed in procambial cells: synthesis of PtdIns(4,5)P2 and PtdIns(3,4,5)P3 in insect cells by 5-phosphorylation of precursors. *Plant J.* **26**, 561-571.
- Furuta, K. M., Yadav, S. R., Lehesranta, S., Belevich, I., Miyashima, S., Heo, J.-o., Vaten, A., Lindgren, O., De Rybel, B., Van Isterdael, G. et al.** (2014). Arabidopsis NAC45/86 direct sieve element morphogenesis culminating in enucleation. *Science* **345**, 933-937.
- Gujas, B., Alonso-Blanco, C. and Hardtke, C. S.** (2012). Natural Arabidopsis brx loss-of-function alleles confer root adaptation to acidic soil. *Curr. Biol.* **22**, 1962-1968.
- Ischebeck, T., Werner, S., Krishnamoorthy, P., Lerche, J., Meijon, M., Stenzel, I., Lofke, C., Wiessner, T., Im, Y. J., Perera, I. Y. et al.** (2014). Phosphatidylinositol 4,5-bisphosphate influences PIN polarization by controlling clathrin-mediated membrane trafficking in Arabidopsis. *Plant Cell* **25**, 4894-4911.
- Kircher, S. and Schopfer, P.** (2012). Photosynthetic sucrose acts as cotyledon-derived long-distance signal to control root growth during early seedling development in Arabidopsis. *Proc. Natl. Acad. Sci. USA* **109**, 11217-11221.
- Lucas, W. J., Groover, A., Lichtenberger, R., Furuta, K., Yadav, S.-R., Helariutta, Y., He, X.-Q., Fukuda, H., Kang, J., Brady, S. M. et al.** (2013). The plant vascular system: evolution, development and functions. *F. J. Integr. Plant Biol.* **55**, 294-388.
- Malamy, J. E. and Benfey, P. N.** (1997). Organization and cell differentiation in lateral roots of Arabidopsis thaliana. *Development* **124**, 33-44.
- Miyashima, S., Sebastian, J., Lee, J.-Y. and Helariutta, Y.** (2013). Stem cell function during plant vascular development. *EMBO J.* **32**, 178-193.
- Mouchel, C. F., Briggs, G. C. and Hardtke, C. S.** (2004). Natural genetic variation in Arabidopsis identifies BREVIS RADIX, a novel regulator of cell proliferation and elongation in the root. *Genes Dev.* **18**, 700-714.
- Mouchel, C. F., Osmont, K. S. and Hardtke, C. S.** (2006). BRX mediates feedback between brassinosteroid levels and auxin signalling in root growth. *Nature* **443**, 458-461.
- Munnik, T. and Nielsen, E.** (2011). Green light for polyphosphoinositide signals in plants. *Curr. Opin. Plant Biol.* **14**, 489-497.
- Munnik, T. and Zarza, X.** (2013). Analyzing plant signaling phospholipids through 32Pi-labeling and TLC. *Methods Mol. Biol.* **1009**, 3-15.
- Nagawa, S., Sawa, S., Sato, S., Kato, T., Tabata, S. and Fukuda, H.** (2006). Gene trapping in Arabidopsis reveals genes involved in vascular development. *Plant Cell Physiol.* **47**, 1394-1405.
- Osmont, K. S., Sibout, R. and Hardtke, C. S.** (2007). Hidden branches: developments in root system architecture. *Annu. Rev. Plant Biol.* **58**, 93-113.
- Péret, B., De Rybel, B., Casimiro, I., Benková, E., Swarup, R., Laplace, L., Beeckman, T. and Bennett, M. J.** (2009). Arabidopsis lateral root development: an emerging story. *Trends Plant Sci.* **14**, 399-408.
- Ragni, L., Nieminen, K., Pacheco-Villalobos, D., Sibout, R., Schwechheimer, C. and Hardtke, C. S.** (2011). Mobile gibberellin directly stimulates Arabidopsis hypocotyl xylem expansion. *Plant Cell* **23**, 1322-1336.
- Robert, H. S. and Friml, J.** (2009). Auxin and other signals on the move in plants. *Nat. Chem. Biol.* **5**, 325-332.
- Rodriguez-Villalon, A., Gujas, B., Kang, Y. H., Breda, A. S., Cattaneo, P., Depuydt, S. and Hardtke, C. S.** (2014). Molecular genetic framework for protophloem formation. *Proc. Natl. Acad. Sci. USA* **111**, 11551-11556.
- Sankar, M., Osmont, K. S., Rolcik, J., Gujas, B., Tarkowska, D., Strnad, M., Xenarios, I. and Hardtke, C. S.** (2011). A qualitative continuous model of cellular auxin and brassinosteroid signaling and their crosstalk. *Bioinformatics* **27**, 1404-1412.
- Santuari, L., Scacchi, E., Rodriguez-Villalon, A., Salinas, P., Dohmann, E. M. N., Brunoud, G., Vernoux, T., Smith, R. S. and Hardtke, C. S.** (2011). Positional information by differential endocytosis splits auxin response to drive Arabidopsis root meristem growth. *Curr. Biol.* **21**, 1918-1923.
- Scacchi, E., Osmont, K. S., Beuchat, J., Salinas, P., Navarrete-Gomez, M., Trigueros, M., Ferrandiz, C. and Hardtke, C. S.** (2009). Dynamic, auxin-responsive plasma membrane-to-nucleus movement of Arabidopsis BRX. *Development* **136**, 2059-2067.
- Scacchi, E., Salinas, P., Gujas, B., Santuari, L., Krogan, N., Ragni, L., Berleth, T. and Hardtke, C. S.** (2010). Spatio-temporal sequence of cross-regulatory events in root meristem growth. *Proc. Natl. Acad. Sci. USA* **107**, 22734-22739.
- Stadler, R., Lauterbach, C. and Sauer, N.** (2005). Cell-to-cell movement of green fluorescent protein reveals post-phloem transport in the outer integument and identifies symplastic domains in Arabidopsis seeds and embryos. *Plant Physiol.* **139**, 701-712.
- Swarup, R., Friml, J., Marchant, A., Ljung, K., Sandberg, G., Palme, K. and Bennett, M.** (2001). Localization of the auxin permease AUX1 suggests two functionally distinct hormone transport pathways operate in the Arabidopsis root apex. *Genes Dev.* **15**, 2648-2653.
- Tejos, R., Sauer, M., Vanneste, S., Palacios-Gomez, M., Li, H., Heilmann, M., van Wijk, R., Vermeer, J. E. M., Heilmann, I., Munnik, T. et al.** (2014). Bipolar plasma membrane distribution of phosphoinositides and their requirement for auxin-mediated cell polarity and patterning in Arabidopsis. *Plant Cell* **26**, 2114-2128.
- Tian, H., De Smet, I. and Ding, Z.** (2014). Shaping a root system: regulating lateral versus primary root growth. *Trends Plant Sci.* **19**, 426-431.
- Truernit, E., Bauby, H., Belcram, K., Barthelemy, J. and Palauqui, J.-C.** (2012). OCTOPUS, a polarly localised membrane-associated protein, regulates phloem differentiation entry in Arabidopsis thaliana. *Development* **139**, 1306-1315.
- Van Norman, J. M., Xuan, W., Beeckman, T. and Benfey, P. N.** (2013). To branch or not to branch: the role of pre-patterning in lateral root formation. *Development* **140**, 4301-4310.